ISSN 1995-0802, Lobachevskii Journal of Mathematics, 2017, Vol. 38, No. 6, pp. 1165–1178. © Pleiades Publishing, Ltd., 2017.
Original Russian Text © V.Yu. Chebakova, 2016, published in Uchenye Zapiski Kazanskogo Universiteta, Seriya Fiziko-Matematicheskie Nauki, 2016, Vol. 158, No. 3, pp. 404–423.

Modeling of Radio-Frequency Capacitive Discharge under Atmospheric Pressure in Argon

V. Yu. Chebakova*

Kazan Federal University, Kazan, 420008 Russia

Received May 31, 2016

Abstract—We consider a one-dimensional self-consistent mathematical model of capacitive radio-frequency discharge in Argon between symmetrical electrodes at atmospheric pressure in the local approximation. The model incorporates electrons, atomic and molecular ions, metastable atoms, Argon dimers, and ground-state atoms. The numerical algorithm for the model is based on a finite-dimensional approximation of the problem using difference schemes with subsequent iterations. A software package in the MatLab environment has been developed to implement the numerical algorithm. Using this software for a model problem, we have obtained the characteristics of a radio-frequency discharge in a plasmatron with interelectrode distances of 0.2 and 2 cm at atmospheric pressure. The results of numerical calculations are in good agreement with data known from literature of field experiments and calculations.

DOI: 10.1134/S1995080217060154

Keywords and phrases: *mathematical modeling, radio-frequency capacitive discharge, discharge at atmospheric pressure, local approximation, numerical experiments*

INTRODUCTION

Low-temperature plasma is widely used in many fields of science and technology [1–6]. Among various types of discharges used to obtain plasma, the radio-frequency discharges (specifically, radio-frequency capacitive (RFC) discharges) have a significant place [7–12]. Argon is often used as a plasma-forming gas. To internal and external parameters of a discharge coupled using experimental calculation techniques that mutually complement each other to solve many problems in physics and chemistry of low-temperature plasma [13, 14]. Our previous papers [15, 16] include a review of studies that address the simulation of RFC discharges. Normally, the studies that consider these discharges in Argon assume that the plasma contains electrons, atomic ions, metastable atoms, and ground-state atoms. However, in was found in a study of the dependence of the ratios of the concentrations of molecular and atomic ions in Argon at atmospheric pressure on the gas temperature [17] that molecular ions are dominant at temperatures of around 500 K and the concentration of atomic ions starts growing at temperatures above 1500 K. Therefore, the papers [18–21] solved model problems that take into account electrons, atomic ions, metastable atoms, and ground-state atoms to analyze the dependence of gas temperature and other discharge characteristics on the boundary conditions describing the properties of the electrode sample and concluded that molecular ions and Argon dimers should be included into the kinetic mechanism.

In this study, we take into account the above-mentioned factors and propose a one-dimensional self-consistent model of RFC discharges at atmospheric pressure in Argon. We developed an approximate algorithm for numerical implementation of the proposed nonlinear model on the basis of its finite-dimensional approximation and subsequent use of the iterative method. It should be noted that various iterative methods for solving nonlinear problems, including problems with partial derivatives, have been proposed earlier (for example, [22–26]). However, the problem considered by us has a number of specific features, such as the difference in time scales of the change in main characteristics of the steady-state low-pressure RFC discharge. In addition, a characteristic feature of the problem is the large gradients of

*E-mail: vchebakova@mail.ru

density of charged particles and electric field strength, and electron temperature in near-electrode layers at the boundaries of the computational domain. Therefore, we had to develop special-purpose methods that take into account these specific features. The results of the numerical experiments conducted by us are qualitatively and quantitatively consistent with the data of field experiments known from the literature and the results of numerical calculations.

1. STATEMENT OF THE PROBLEM

We consider an RFC-discharge between two plane-parallel electrodes one of which is grounded and the other is linked with an RFC-generator; the distance between the electrodes is smaller than the dimensions of the electrodes themselves. Under these conditions, the electric field is close to the potential field and the discharge is homogeneous along the electrodes. This makes it possible to use a one-dimensional model allowing the kinetics of plasma-chemical processes to be taken into account in the diffusion–drift formulation. The estimates for the time and distance at which the electrons lose the energy acquired from the field indicate that the RFC-discharge at atmospheric pressures can be simulated using a local approximation ensuring that the parameters of the electronic component of plasma (such as the coefficients of diffusion and mobility, mean energy, and plasma-chemical reaction rates) depend on the local value of the reduced electric field (the ratio E/N of the electric field intensity E to the concentration of heavy particles N—the concentration of the Argon atoms in the ground state) [27]. This model takes into account the following features of the RFC-discharge: there are regions with no quasi-neutrality, the applied stress varies in time, and there are processes involving metastable atoms, molecular ions, and dimers. The efficient mixing of the four lower closely spaced electronic excited states allows them to be replaced with a single level [28, 29].

By b, we denote the distance between the electrodes, assuming that the grounded and loaded electrodes are located at $x = 0$ and $x = b$ (the Ox-axis is perpendicular to the surface of the electrodes).

The processes occurring in an RFC-discharge at atmospheric pressures can be described using the following initial–boundary value problems and Cauchy problems.

1.1. Convection–Diffusion Equation for Atomic Ions

$$\frac{\partial n_+}{\partial t} + \frac{\partial G_+}{\partial x} = R_1 n_e N + R_2 n_m^2 + R_3 n_m n_e - R_5 n_+ n_e^2 - R_4 n_+ n_e + R_{12} n_e n_{2+} - R_{11} n_+ N^2 + R_{20} N n_{2+}, \quad 0 < x < b, \quad t > 0, \tag{1}$$

where n_e and n_{2+} are the concentrations of electrons and atomic and molecular positively charged ions, respectively; n_m is the effective concentration of metastable Argon atoms; $G_+ = -D_+ \partial n_+/\partial x + n_+ \mu_+ E$ is the atomic ion flux density; μ_+ is the mobility of atomic ions; D_+ is the coefficient of diffusion of atomic ions; and $E = \partial\varphi/\partial x$, φ is the electric field potential.

Hereafter, R_i, $i = 1, 2, \ldots, 20$ are the rate coefficients of plasma-chemical reactions (see Table 1).

In line with [28], we supplement Eq. (1) with the following boundary conditions:

for $x = 0$

$$\begin{cases} G_+(0,t) = (-n_+ v_+ + \mu_+ n_+ E)|_{(0+,t)}, & E < 0, \\ G_+(0,t) = (-n_+ v_+)|_{(0+,t)}, & E \geq 0; \end{cases} \tag{2}$$

for $x = b$

$$\begin{cases} G_+(b,t) = (n_+ v_+ + \mu_+ n_+ E)|_{(b-,t)}, & E \geq 0, \\ G_+(b,t) = (n_+ v_+)|_{(b-,t)}, & E < 0. \end{cases} \tag{3}$$

Here, m_+ is the atomic ion mass, $v_+ = \sqrt{8kT_a/(\pi m_+)}/4$ is the average thermal velocity of atomic ions, and k is the Boltzmann constant.

The model assumes that the temperatures T_a of atoms, atomic ions, and excited atoms are the same, which is reflected in the formulation of boundary conditions (2)–(3) and (5), (6), and (13) below.

1.2. Convection–Diffusion Equation for Molecular Ions Ar_{2+}

$$\frac{\partial n_{2+}}{\partial t} + \frac{\partial G_{2+}}{\partial x} = R_{10}n_m^2 + R_{11}n_+N^2 - R_{13}n_{2+}n_e + R_{16}n_{2*}^2 + R_{17}n_mn_{2*} - R_{20}Nn_{2+}, \quad 0 < x < b, \quad t > 0, \tag{4}$$

where n_{2*} is the concentration of Argon dimers, $G_{2+} = -D_{2+}\partial n_{2+}/\partial x + n_{2+}\mu_{2+}E$ is the molecular ion flux density, μ_{2+} is the mobility of molecular ions, and D_{2+} is the diffusion coefficient of molecular ions.

Like in the convection–diffusion equation for atomic ions, we formulate the boundary conditions in the following way (m_{2+} is the mass of a positively charged molecular ion):

for $x = 0$

$$\begin{cases} G_{2+}(0,t) = \left(-n_{2+}v_{2+} + \mu_{2+}n_{2+}E\right)|_{(0+,t)}, & E < 0, \\ G_{2+}(0,t) = \left(-n_{2+}v_{2+}\right)|_{(0+,t)}, & E \geq 0; \end{cases} \tag{5}$$

for $x = b$

$$\begin{cases} G_{2+}(b,t) = \left(n_{2+}v_{2+} + \mu_{2+}n_{2+}E\right)|_{(b-,t)}, & E \geq 0, \\ G_{2+}(b,t) = \left(n_{2+}v_{2+}\right)|_{(b-,t)}, & E < 0, \end{cases} \tag{6}$$

where $v_{2+} = \sqrt{8kT_a/(\pi m_{2+})}/4$ is the average thermal velocity of molecular ions.

1.3. Convection–Diffusion Equation for an Electron Gas

$$\frac{\partial n_e}{\partial t} + \frac{\partial G_e}{\partial x} = R_1n_eN + R_2n_m^2 + R_3n_mn_e - R_4n_en_+ - R_5n_+n_e^2 + R_{10}n_m^2 - R_{13}n_{2+}n_e + R_{16}n_{2*}^2 + R_{17}n_mn_{2*}, \quad 0 < x < b, \quad t > 0, \tag{7}$$

where $G_e = -D_e\partial n_e/\partial x - n_e\mu_eE$ is the electron flux density, μ_e is the electron mobility, and D_e is the diffusion coefficient of the electrons.

The boundary conditions for $x = 0$ are taken as

$$\begin{cases} G_e(0,t) = \left(-n_ev_e - \mu_en_eE\right)|_{(0+,t)}, & E \geq 0, \\ G_e(0,t) = \left(-n_ev_e - \gamma(\mu_+n_+E + \mu_{2+}n_{2+}E)\right)|_{(0+,t)}, & E < 0; \end{cases} \tag{8}$$

and, for $x = b$, as

$$\begin{cases} G_e(b,t) = \left(n_ev_e - \mu_en_eE\right)|_{(b-,t)}, & E < 0, \\ G_e(b,t) = \left(n_ev_e - \gamma(\mu_+n_+E + \mu_{2+}n_{2+}E)\right)|_{(b-,t)}, & E \geq 0. \end{cases} \tag{9}$$

Here, γ is the secondary electron emission coefficient from electrodes, T_e is the temperature of electrons, m_e is the mass of electrons, and $v_e = \sqrt{8kT_e/(\pi m_e)}/4$ is the average thermal velocity of electrons.

Under normal conditions, it is assumed that the gas contains $\sim 10^4$ cm^{-3} charged particles. This value is taken as the initial condition for the total concentration of charged positive particles and electrons.

1.4. The Poisson Equation for the Electric Field Potential

$$-\frac{\partial^2\varphi}{\partial x^2} = \frac{q_e}{\varepsilon_0}\left(n_+ + n_{2+} - n_e\right), \quad 0 < x < b, \quad t > 0, \tag{10}$$

with boundary values

$$\begin{cases} \varphi(b,t) = V_a\sin(\omega t) \quad \text{(loaded electrode)}, \\ \varphi(0,t) = 0 \quad \text{(grounded electrode)}. \end{cases} \tag{11}$$

Here, q_e is the electron charge, ε_0 is the electric constant of the vacuum, ω is the circular frequency of the electromagnetic field, and V_a is the amplitude of the voltage oscillation on the loaded electrode.

1.5. Equation of Balance of the Concentration of Metastable Atoms

$$\frac{\partial n_m}{\partial t} - \frac{\partial G_m}{\partial x} = R_6 n_e N + R_{18} n_e n_{2*} - R_2 n_m^2 - R_3 n_m n_e - R_7 n_m - R_8 n_m N - R_9 n_m n_e - R_{10} n_m^2 - R_{15} n_m N^2 - R_{17} n_m n_{2*} - R_{19} n_m N^2, \quad 0 < x < b, \quad t > 0. \tag{12}$$

Here, $G_m = D_m \partial n_m / \partial x$ is the density of the flux of metastable atoms and D_m is the coefficient of diffusion of metastable Argon atoms.

The boundary conditions for Eq. (12) are

$$\begin{cases} G_m(0,t) = (-n_a v_a)|_{(0+,t)}, \\ G_m(b,t) = (n_a v_a)|_{(b-,t)}, \end{cases} \tag{13}$$

where $v_a = \sqrt{8kT_a/(\pi m_a)}/4$ is the average thermal velocity of excited atoms.

The initial conditions for Eq. (12) are given as

$$n_m(x,0) = 0. \tag{14}$$

1.6. Kinetic Equation for Argon Dimers Ar_2^*

$$\frac{\partial n_{2*}}{\partial t} = R_{19} n_m N^2 + R_{15} N^2 n_m - R_{14} n_{2*} - R_{16} n_{2*}^2 - R_{17} n_m n_{2*} - R_{18} n_e n_{2*}. \tag{15}$$

We take the initial conditions to be zero like for metastable atoms:

$$n_{2*}(x,0) = 0. \tag{16}$$

1.7. Kinetic Equation for Neutral Atoms

$$\frac{\partial N}{\partial t} = -R_1 n_e N + R_2 n_m^2 + R_4 n_+ n_e + R_5 n_+ n_e^2 - R_6 n_e N + R_7 n_m + R_8 n_m N + R_9 n_m n_e - R_{11} n_+ N^2 + R_{12} n_{2+} n_e + 2R_{13} n_{2+} n_e + R_{14} n_{2*} - R_{15} n_m N^2 + 2R_{16} n_{2*} + R_{17} n_m n_{2*} - R_{19} n_m N^2, \quad 0 < x < b, \quad t > 0. \tag{17}$$

Based on the equation of an ideal gas, we use the following initial conditions: $P/(kT_a(x,0)) = N(x,0)$.

1.8. Equation of Thermal Conductivity of an Atomic-Ion Gas

Due to the fact that the fluctuations of the atomic temperature near the values averaged over the field variation time are negligibly small, the equation of atomic temperature balance can be considered as averaged over the period of electric field oscillation determined by the frequency $f = 13.56$ MHz of the high-frequency generator. In addition, we assume that the coefficient of transfer of the energy received by ions during their movement to atoms due to the field is unity [11]. This should not lead to a significant overestimation of atomic temperature because the energy received from collisions of atoms and electrons is much larger than the energy received from collisions of atoms and ions.

Hereafter, we denote the averaging of a relevant quantity over the period $T = 2\pi/\omega = 1/f$, where $\omega = 2\pi f$ is the circular frequency of the generator. For example, we assume for n_e at $t \in ((p-1)T, pT]$, $p = 1, 2, \ldots$ (p is the period number) that

$$\widehat{n}_e^p(x) = \int\limits_{(p-1)T}^{pT} n_e(x,\xi) d\xi. \tag{18}$$

Similarly, we can average other parameters entering into the equation of heat conduction of an atomic-ion gas. In view of the above discussion, this equation for $t \in ((p-1)T, pT]$, $p = 1, 2, \ldots$ has the form

$$\frac{\partial}{\partial x}\left(-\lambda_a \frac{\partial T_a}{\partial x}\right) = \widehat{j}_i^{\,p}\widehat{E}^p + \widehat{Q}_{\rm el}^{\,p}\widehat{n}_e^{\,p}\widehat{N}^p, \tag{19}$$

where $j_i = q_e(G_+ + G_{2+})$ is the ion current, λ_a is the coefficient of thermal conductivity of an atomic-ion gas, and $Q_{\rm el}$ is the energy obtained by heavy particles in elastic collisions.

We assume that the electrode is cooled by water. Then, Eq. (19) is supplemented by the boundary conditions

$$\begin{aligned} -\lambda_a \frac{\partial T_a(0)}{\partial x} &= -\chi\left(T_a(0) - T_{\rm W}\right), \\ -\lambda_a \frac{\partial T_a(b)}{\partial x} &= \chi\left(T_a(b) - T_{\rm W}\right), \end{aligned} \tag{20}$$

where χ is the total heat transfer coefficient of the sample and $T_{\rm W}$ is the temperature of the water that cools the electrode.

1.9. Characteristics of Processes

The calculations were performed using the SI system of measurement units. The data for approximating the diffusion coefficient D_e, electron mobility μ_e, the rate coefficients for direct ionization R_1 and metastable excitation R_6, the contribution induced by elastic collisions to the gas heating $Q_{\rm el}$, and mean energy $\overline{\varepsilon} = 3kT_e/2$ are chosen taking into account their dependence on the reduced electric field intensity and electron–electron collisions using the BOLSIG + software package, version 1.2 [31]. For convenience, these and the remaining dependencies are summarized in Table 1.

2. DIFFERENCE SCHEMES FOR BOUNDARY VALUE, INITIAL–BOUNDARY VALUE, AND CAUCHY PROBLEMS IN THE SYSTEM

The numerical algorithm for modeling the RFC-discharge at increased pressures is well similar to the algorithm for the problem at low pressures described in [18] and based on the removal of nonlinearity with respect to the coefficients on the lower layer. The nonlinear quadratic terms on the right-hand side were linearized using the Newton scheme [46]. The equation for gas temperature was solved once for the period T using a Jacobi-type iterative process.

On the interval $[0, b]$, we introduce the three-dimensional uniform grids $\omega_h = \{x_l = lh, l = 1, 2, \ldots, M-1\}$, $\overline{\omega}_h = \{x_l = lh, l = 0, 1, \ldots, M\}$, $h = b/M$, as well as the time grid $\omega_\tau = \{t_s = s\tau, s = 0, 1, \ldots\}$, where $\tau = T/L_T$ is the time step and L_T is the number of time steps per period. On the grids $\omega_h \times \omega_\tau$ and $\overline{\omega}_h$, we define grid functions with the same notations as for the differential functions. We denote the values of the grid functions φ at the point $x_l^s = (x_l, t_s) \in \overline{\omega}_h \times \omega_\tau$ by φ_l^s.

2.1. Difference Scheme for the Problem of Balance of Atomic Ions

At $s > 0$ and $2 \le l \le M-2$, the difference scheme for problem (1)–(3) has the form

$$\begin{aligned} h\frac{n_{+,l}^s - n_{+,l}^{s-1}}{\tau} - \left(D_{+,l+1/2}^{s-1}\frac{n_{+,l+1}^s - n_{+,l}^s}{h} - D_{+,l-1/2}^{s-1}\frac{n_{+,l}^s - n_{+,l-1}^s}{h}\right) \\ - E_{l-1/2}^{+,s-1}\mu_{+,l-1}^{s-1}n_{+,l-1}^s + E_{l+1/2}^{-,s-1}\mu_{+,l+1}^{s-1}n_{+,l+1}^s + E_{l+1/2}^{+,s-1}\mu_{+,l}^{s-1}n_{+,l}^s \\ - E_{l-1/2}^{-,s-1}\mu_{+,l}^{s-1}n_{+,l}^s = h\Big(R_{1,l}^{s-1}n_{e,l}^{s-1}N_l^{s-1} + R_{2,l}^{s-1}\Big(n_{m,l}^{s-1}\Big)^2 + R_{3,l}^{s-1}n_{m,l}^{s-1}n_{e,l}^{s-1} \\ - R_{4,l}^{s-1}n_{e,l}^{s-1}n_{+,l}^s - R_{5,l}^{s-1}\Big(n_{e,l}^{s-1}\Big)^2 n_{+,l}^s + R_{12,l}^{s-1}n_{e,l}^{s-1}n_{2+,l}^{s-1} \\ - R_{11,l}^{s-1}n_{+,l}^{s-1}\Big(N_{2+l}^{s-1}\Big)^2 + R_{20,l}^{s-1}n_{2+,l}^{s-1}N_l^{s-1}\Big). \end{aligned}$$

Table 1

No.	Process/characteristic	Value of parameter	Source
1	Direct ionization $Ar + e \to Ar^+ + 2e$	R_1 is calculated using BOLSIG+, version1.2	[31]
2	Penning ionization $Ar^* + Ar^* \to Ar + Ar^+ + e$	$R_2 = \text{const} = 6.2 \times 10^{-16}$ $R_2 = 7 \times 10^{-16}(T_a/300)^{0.5}$ $R_2 = 1.2 \times 10^{-15}(T_a/300)^{0.5}$ $R_2 = \text{const} = 5 \times 10^{-16}$	[32] [33] [34, 35] [36]
3	Stepwise ionization $Ar^* + e \to Ar^+ + 2e$	$R_3 = 2 \times 10^{-11} \exp(-25524.4/T_e)$	[33]
4	Photo-recombination $Ar^+ + e \to Ar + h_\nu$	$R_4 = 2.7 \times 10^{-19}(T_e/11602)^{-3/4}$	[13]
5	Ternary recombination $Ar^+ + 2e \to Ar + e$	$R_5 = 8.75 \times 10^{-39}(T_e/11602)^{-9/2}$	[13]
6	Excitation of metastable atoms $Ar + e \to Ar^* + e$	R_6 is calculated using BOLSIG+, version 1.2 $R_6 = 10^{-9}(T_e/11602)\times$ $\times \exp(-134583/T_e)$	[31] [13]
7	Radiation $Ar^* \to Ar + h_\nu$	$R_7 = \text{const} = 2.5 \times 10^{-11}$ $R_7 = \text{const} = 5 \times 10^{-11}$	[29] [34, 35]
8	$Ar^* + Ar \to 2Ar$	$R_8 = \text{const} = 3 \times 10^{-21}$	[32]
9	$Ar^* + e \to Ar + e$	$R_9 = \text{const} = 10^{-11}$	[32]
10	Chemoionization $Ar^* + Ar^* \to Ar_{2+} + e$	$R_{10} = \text{const} = 1.2 \times 10^{-11}$	[29]
11	Ion conversion $2\,Ar + Ar^+ \to Ar_{2+} + Ar$	$R_{11} = \text{const} = 2.5 \times 10^{-43}$ $R_{11} = 2.25 \times 10^{-43}(T_a/300)^{-0.4}$ $R_{11} = 2.5 \times 10^{-43}(T_a/300)^{3/2}$ $R_{11} = 2.5 \times 10^{-43}$	[29] [17] [34, 35] [36]
12	$Ar_{2+} + e \to Ar + Ar^+ + e$	$R_{12} = 1 \times 10^{-11} \exp(-23204/T_e)$	[33]
13	$Ar_{2+} + e \to Ar + Ar$	$R_{13} = 1 \times 10^{-13}T_e^{-0.6}(T_a/300)^{-0.6}$ $R_{13} = 1.1 \times 10^{-13}(T_e/11602)^{-0.5}$	[33] [37]
14	$Ar_2^* \to 2Ar + h_\nu$	$R_{14} = \text{const} = 1 \times 10^{-11}$	[33]
15	$Ar^* + 2Ar \to Ar_2^* + Ar$	$R_{15} = \text{const} = 1.1 \times 10^{-43}$	[32, 38]
16	$Ar_2^* + Ar_2^* \to e + 2Ar + Ar_{2+}$	$R_{16} = 7 \times 10^{-16}(T_a/300)^{0.5}$	[33]
17	$Ar_2^* + Ar^* \to e + Ar + Ar_{2+}$	$R_{17} = 7 \times 10^{-16}(T_a/300)^{0.5}$	[33]
18	$e + Ar_2^* \to 2\,Ar^* + e$	$R_{18} = 1 \times 10^{-13} \exp(11602/T_e)$	[33]
19	Dimer formation $Ar^* + 2\,Ar \to Ar_2^* + Ar$	$R_{19} = \text{const} = 1.5 \times 10^{-44}$	[29]
20	$Ar_2^* + Ar \to 3Ar + Ar^* + e$	$R_{20} = \dfrac{5.22 \times 10^{-16} \exp(-15129.008/T_a)}{T_a/11602}$	[33]
21	Ion diffusion coefficient	$D_+ = 1 \times 10^{23}(T_a)^{1/2}/N$ $D_+ = 2.07 \times 10^{20}/N$ $D_+ = 0.11029 \times 10^{25}/N$	[17] [32] [39]
22	Molecular ion mobility	$\mu_{2+} = 1.79 \times (T_a/300)$	[40]
23	Thermal conductivity of atomic-ion gas	$\lambda_a = 3.5 \times 10^{-4}(T_a^{0.68})$ $\lambda_a = 1.78 \times 10^{-2}(T_a/300)^{0.66}$	[33] [41, p. 61]

Table 1. (Contd.)

No.	Process/characteristic	Value of parameter	Source
24	Atomic ion mobility	$\mu_+ = 4.65 \times 10^{20}/N$ $\mu_+ = 0.044/T_a$ $\mu_+ = \mu_{[43]}$ [1)]	[32] [42] [43]
25	Coefficient of diffusion of metastable atoms	$D_m = 0.18023 \times 10^{20}/N$ $D_m = 2.42 \times 10^{20}/N$	[39] [32]
26	Coefficient of diffusion	D_e is calculated using) BOLSIG+, version 1.2	[31]
27	Mobility of electrons	μ_e is calculated using BOLSIG+, version 1.2	[31]
28	Energy received by heavy particles at elastic collisions	Q_{el} is calculated using BOLSIG+, version 1.2	[31]
29	Coefficient of diffusion of molecular ion	$D_{2+} = 0.13181 \times 10^{25}/N$	[44, 45]
30	$\mathrm{Ar}_2^* + \mathrm{e} \to \mathrm{Ar}^* + \mathrm{Ar}$	$7 \times 10^{-13}(T_e/300N)^{-0.5}$	[34, 35]

[1)] The mobility of atomic ions $\mu_{[43]}$ is calculated from the relation

$$\left(\frac{P}{133}\right)\mu_{[43]} = \begin{cases} 10^{-1}\left(1 - 2.22 \times 10^{-5}\dfrac{E}{P/133}\right), & E/P \le 45; \\ \dfrac{8.25 \times 10^3}{\left(\dfrac{E/100}{P/133}\right)^{1/2}} \dfrac{\left(\dfrac{E/100}{P/133}\right)^{3/2} - 86.52}{\left(\dfrac{E/100}{P/133}\right)^{3/2}}, & E/P > 45. \end{cases}$$

Hereafter, $E^{\pm} = (E \pm |E|)/2$ are the positive and negative components of the field E.

Boundary conditions (2)–(3) are approximated as follows. At $s > 0$ and $l = 1$, we have

$$h\frac{n_{+,1}^s - n_{+,1}^{s-1}}{\tau} - D_{+,3/2}^{s-1}\frac{n_{+,2}^s - n_{+,1}^s}{h} + \left(E_{1/2} + E_{3/2}\right)^{+,s-1}\mu_{+,1}^{s-1}n_{+,1}^s/2$$
$$+ \left(E_{5/2} + E_{3/2}\right)^{-,s-1}\mu_{+,2}^{s-1}n_{+,2}^s/2 - \Big[-\frac{1}{4}n_{+,1}^s\sqrt{8kT_{a,1}/\pi m_+}$$
$$+ \left(E_{1/2} + E_{3/2}\right)^{-,s-1}\mu_{+,1}^{s-1}n_{+,1}^s/2\Big] = h\Big(R_{1,1}^{s-1}n_{e,1}^{s-1}N_1^{s-1} + R_{2,1}^{s-1}\left(n_{m,1}^{s-1}\right)^2$$
$$+ R_{3,1}^{s-1}n_{m,1}^{s-1}n_{e,1}^{s-1} - R_{4,1}^{s-1}n_{e,1}^{s-1}n_{+,1}^s - R_{5,1}^{s-1}\left(n_{e,1}^{s-1}\right)^2 n_{+,1}^s + R_{12,1}^{s-1}n_{e,1}^{s-1}n_{2+,1}^{s-1}$$
$$- R_{11,1}^{s-1}n_{+,1}^{s-1}\left(N_1^{s-1}\right)^2 + R_{20,1}^{s-1}n_{2+,1}^{s-1}N_1^{s-1}\Big).$$

At $s > 0$ and $l = M - 1$, we have

$$h\frac{n_{+,M-1}^s - n_{+,M-1}^{s-1}}{\tau} - \Big[-D_{+,M-3/2}^{s-1}\frac{n_{+,M-1}^s - n_{+,M-2}^s}{h}$$
$$+ \left(E_{M-1/2} + E_{M-3/2}\right)^{-,s-1}\mu_{+,M-1}^{s-1}n_{+,M-1}^s/2 + \left(E_{5/2} + E_{3/2}\right)^{-,s-1}\mu_{+,M-2}^{s-1}n_{+,M-2}^s/2\Big]$$
$$+ \frac{1}{4}n_{+,M-1}^s\sqrt{8kT_{a,M-1}/\pi m_+} + \left(E_{M-1/2} + E_{M-3/2}\right)^{+,s-1}\mu_{+,M-1}^{s-1}n_{+,M-1}^s/2$$
$$= h\Big(R_{1,M-1}^{s-1}n_{e,M-1}^{s-1}N_{M-1}^{s-1} + R_{2,M-1}^{s-1}\left(n_{m,M-1}^{s-1}\right)^2 + R_{3,M-1}^{s-1}n_{m,M-1}^{s-1}n_{e,M-1}^{s-1}$$

$$- R^{s-1}_{4,M-1}n^{s-1}_{e,M-1}n^{s}_{+,M-1} - R^{s-1}_{5,M-1}\Big(n^{s-1}_{e,M-1}\Big)^2 n^{s}_{+,M-1} + R^{s-1}_{12,M-1}n^{s-1}_{e,M-1}n^{s-1}_{2+,M-1}$$
$$- R^{s-1}_{11,M-1}n^{s-1}_{+,M-1}\Big(N^{s-1}_{M-1}\Big)^2 + R^{s-1}_{20,M-1}n^{s-1}_{2+,M-1}N^{s-1}_{M-1}\Big).$$

2.2. Difference Scheme for the Problem of Balance of Molecular Ions

At $s > 0$ and $2 \le l \le M-2$, the difference scheme for problem (4)–(6) has the form

$$h\frac{n^{s}_{2+,l} - n^{s-1}_{2+,l}}{\tau} - \left(D^{s-1}_{2+,l+1/2}\frac{n^{s}_{2+,l+1} - n^{s}_{2+,l}}{h} - D^{s-1}_{2+,l-1/2}\frac{n^{s}_{2+,l} - n^{s}_{2+,l-1}}{h}\right)$$
$$- E^{+,s-1}_{l-1/2}\mu^{s-1}_{2+,l-1}n^{s}_{2+,l-1} + E^{-,s-1}_{l+1/2}\mu^{s-1}_{2+,l+1}n^{s}_{2+,l+1} + E^{+,s-1}_{l+1/2}\mu^{s-1}_{2+,l}n^{s}_{2+,l}$$
$$- E^{-,s-1}_{l-1/2}\mu^{s-1}_{2+,l}n^{s}_{2+,l} = h\Big(R^{s-1}_{10,l}\Big(n^{s-1}_{m,l}\Big)^2 + R^{s-1}_{11,l}\Big(N^{s-1}_{l}\Big)^2 n^{s-1}_{+,l} - R^{s-1}_{12,l}n^{s}_{2+,l}n^{s-1}_{e,l}$$
$$- R^{s-1}_{13,l}n^{s-1}_{e,l}n^{s}_{2+,l} + R^{s-1}_{16,l}\Big(n^{s-1}_{2^*,l}\Big)^2 + R^{s-1}_{17,l}n^{s-1}_{m,l}n^{s-1}_{2^*,l} - R^{s-1}_{20,l}n^{s}_{2+,l}N^{s-1}_{l}\Big).$$

Boundary conditions (5)–(6) are approximated as follows. At $s > 0$ and $l = 1$, we have

$$h\frac{n^{s}_{2+,1} - n^{s-1}_{2+,1}}{\tau} - D^{s-1}_{2+,3/2}\frac{n^{s}_{2+,2} - n^{s}_{2+,1}}{h} + \Big(E_{1/2} + E_{3/2}\Big)^{+,s-1}\mu^{s-1}_{2+,1}n^{s}_{2+,1}/2$$
$$+\Big(E_{5/2} + E_{3/2}\Big)^{-,s-1}\mu^{s-1}_{2+,2}n^{s}_{2+,2}/2 + \frac{1}{4}n^{s}_{2+,1}\sqrt{8kT_{a,1}/\pi m_{2+}}$$
$$- \Big(E_{1/2} + E_{3/2}\Big)^{-,s-1}\mu^{s-1}_{2+,1}n^{s}_{2+,1}/2 = h\Big(R^{s-1}_{10,1}\Big(n^{s-1}_{m,1}\Big)^2 + R^{s-1}_{11,1}\Big(N^{s-1}_{1}\Big)^2 n^{s}_{+,1}$$
$$- R^{s-1}_{12,1}n^{s}_{2+,1}n^{s-1}_{e,1} - R^{s-1}_{13,1}n^{s-1}_{e,1}n^{s}_{2+,1} + R^{s-1}_{16,1}\Big(n^{s-1}_{2^*,1}\Big)^2$$
$$+ R^{s-1}_{17,1}n^{s-1}_{m,1}n^{s-1}_{2^*,1} - R^{s-1}_{20,1}n^{s}_{2+,1}N^{s-1}_{1}\Big).$$

At $s > 0$ and $l = M-1$, we have

$$h\frac{n^{s}_{2+,M-1} - n^{s-1}_{2+,M-1}}{\tau} + D^{s-1}_{2+,M-3/2}\frac{n^{s}_{2+,M-1} - n^{s}_{2+,M-2}}{h}$$
$$- \Big(E_{M-1/2} + E_{M-3/2}\Big)^{-,s-1}\mu^{s-1}_{2+,M-1}n^{s}_{2+,M-1}/2$$
$$- \Big(E_{5/2} + E_{3/2}\Big)^{+,s-1}\mu^{s-1}_{2+,M-2}n^{s}_{2+,M-2}/2$$
$$+ \frac{1}{4}n^{s}_{2+,M-1}\sqrt{8kT_{a,M-1}/\pi m_{2+}} + \Big(E_{M-1/2} + E_{M-3/2}\Big)^{+,s-1}\mu^{s-1}_{2+,M-1}n^{s}_{2+,M-1}/2$$
$$= h\Big(R^{s-1}_{10,M-1}\Big(n^{s-1}_{m,M-1}\Big)^2 + R^{s-1}_{11,M-1}\Big(N^{s-1}_{M-1}\Big)^2 n^{s}_{+,M-1} - R^{s-1}_{12,M-1}n^{s}_{2+,M-1}n^{s-1}_{e,M-1}$$
$$- R^{s-1}_{13,M-1}n^{s-1}_{e,M-1}n^{s}_{2+,M-1} - R^{s-1}_{20,M-1}n^{s}_{2+,M-1}N^{s-1}_{M-1} + R^{s-1}_{16,M-1}\Big(n^{s-1}_{2^*,M-1}\Big)^2$$
$$+ R^{s-1}_{17,M-1}n^{s-1}_{m,M-1}n^{s-1}_{2^*,M-1}\Big).$$

2.3. Difference Scheme for the Problem of Electron Gas Balance

At $s > 0$ and $2 \le l \le M-2$, the difference scheme for problem (7)–(9) has the form

$$h\frac{n^{s}_{e,l} - n^{s-1}_{e,l}}{\tau} - \left(D^{s-1}_{e,l+1/2}\frac{n^{s}_{e,l+1} - n^{s}_{e,l}}{h} - D^{s-1}_{e,l-1/2}\frac{n^{s}_{e,l} - n^{s}_{e,l-1}}{h}\right)$$
$$- (-E)^{+,s-1}_{l-1/2}\mu^{s-1}_{e,l-1}n^{s}_{2+,l-1} + (-E)^{-,s-1}_{l+1/2}\mu^{s-1}_{e,l+1}n^{s}_{e,l+1} + (-E)^{+,s-1}_{l+1/2}\mu^{s-1}_{e,l}n^{s}_{e,l}$$

$$- (-E)^{-,s-1}_{l-1/2}\mu^{s-1}_{e,l}n^s_{e,l} = h\Big(R^{s-1}_{1,l}n^{s-1}_{e,l}N^{s-1}_l + R^{s-1}_{3,l}n^{s-1}_{m,l}n^s_{e,l} - R^{s-1}_{4,l}n^s_{+,l}n^s_{e,l}$$
$$- R^{s-1}_{5,l}\Big(\Big(n^{s-1}_{e,l}\Big)^2 n^s_{+,l} + 2n^{s-1}_{e,l}\Big(n^s_{e,l} - n^{s-1}_{e,l}\Big)\Big) - R^{s-1}_{13,l}n^s_{e,l}n^s_{2+,l} + R^{s-1}_{16,l}\Big(n^{s-1}_{2^*,l}\Big)^2$$
$$+ R^{s-1}_{10,l}\Big(n^{s-1}_{m,l}\Big)^2 + R^{s-1}_{17,l}n^{s-1}_{m,l}n^{s-1}_{2^*,l} + R^{s-1}_{2,l}\Big(n^{s-1}_{m,l}\Big)^2\Big).$$

Boundary conditions (8)–(9) are approximated as follows. At $s > 0$ and $l = 1$, we have

$$h\frac{n^s_{e,1} - n^{s-1}_{e,1}}{\tau} - D^{s-1}_{e,3/2}\frac{n^s_{e,2} - n^s_{e,1}}{h} + \Big(-E_{1/2} - E_{3/2}\Big)^{+,s-1}\mu^{s-1}_{e,1}n^s_{e,1}/2$$
$$+ \Big(-E_{5/2} - E_{3/2}\Big)^{-,s-1}\mu^{s-1}_{e,2}n^s_{e,2}/2 + \frac{1}{4}n^s_{e,1}\sqrt{8kT_{e,1}/\pi m_e}$$
$$- \Big(-E_{1/2} - E_{3/2}\Big)^{-,s-1}, \mu^{s-1}_{e,2}n^s_{e,2}/2 = h\Big(R^{s-1}_{1,1}n^s_{e,1}N^{s-1}_1 + R^{s-1}_{2,1}\Big(n^{s-1}_{m,1}\Big)^2$$
$$+ R^{s-1}_{10,1}\Big(n^{s-1}_{m,1}\Big)^2 + R^{s-1}_{3,1}n^{s-1}_{m,1}n^s_{e,1} - R^{s-1}_{4,1}n^s_{e,1}n^s_{+,1} - R^{s-1}_{5,1}\Big(\Big(n^{s-1}_{e,1}\Big)^2$$
$$+ 2n^{s-1}_{e,1}\Big(n^s_{e,1} - n^{s-1}_{e,1}\Big)\Big) + R^{s-1}_{17,1}n^{s-1}_{m,1}n^{s-1}_{2^*,1} - R^{s-1}_{13,1}n^s_{e,1}n^s_{2+,1} + R^{s-1}_{16,1}\Big(n^{s-1}_{2^*,1}\Big)^2\Big)$$
$$- \gamma\Big(E_{1/2} + E_{3/2}\Big)^{-,s-1}\mu^{s-1}_{+,1}n^s_{+,1}/2 - \gamma\Big(E_{1/2} + E_{3/2}\Big)^{-,s-1}\mu^{s-1}_{2+,1}n^s_{2+,1}/2.$$

At $s > 0$ and $l = M - 1$, we have

$$h\frac{n^s_{e,M-1} - n^{s-1}_{e,M-1}}{\tau} + D^{s-1}_{e,M-3/2}\frac{n^s_{e,M-1} - n^s_{e,M-2}}{h}$$
$$- \Big(-E_{M-1/2} - E_{M-3/2}\Big)^{-,s-1}\mu^{s-1}_{e,M-1}n^s_{e,M-1}/2$$
$$- \Big(-E_{5/2} - E_{3/2}\Big)^{+,s-1}\mu^{s-1}_{e,M-2}n^s_{e,M-2}/2 + \frac{1}{4}n^s_{e,M-1}\sqrt{8kT_{e,M-1}/\pi m_e}$$
$$- \Big(-E_{M-1/2} - E_{M-3/2}\Big)^{+,s-1}\mu^{s-1}_{e,M-1}n^s_{e,M-1}/2$$
$$= h\Big(R^{s-1}_{1,M-1}n^s_{e,M-1}N^{s-1}_{M-1} + R^{s-1}_{2,M-1}\Big(n^{s-1}_{m,M-1}\Big)^2 + R^{s-1}_{3,M-1}n^{s-1}_{m,M-1}n^s_{e,M-1}$$
$$- R^{s-1}_{4,M-1}n^{s-1}_{e,M-1}n^s_{+,M-1} - R^{s-1}_{5,M-1}n^s_{+,M-1}\Big(n^{s-1}_{e,M-1}\Big)^2 + R^{s-1}_{10,M-1}\Big(n^{s-1}_{m,M-1}\Big)^2$$
$$+ 2n^{s-1}_{e,M-1}\Big(n^s_{e,M-1} - n^{s-1}_{e,M-1}\Big) - R^{s-1}_{13,M-1}n^s_{e,M-1}n^{s-1}_{2+,M-1}$$
$$+ R^{s-1}_{16,M-1}\Big(n^{s-1}_{2^*,M-1}\Big)^2 + R^{s-1}_{17,M-1}n^{s-1}_{m,M-1}n^{s-1}_{2^*,M-1}\Big)$$
$$+ \gamma\Big(E_{M-1/2} + E_{M-3/2}\Big)^{+,s-1}\mu^{s-1}_{+,M-1}n^s_{+,M-1}/2$$
$$+ \gamma\Big(E_{M-1/2} + E_{M-3/2}\Big)^{-,s-1}\mu^{s-1}_{2+,M-1}n^s_{2+,M-1}/2.$$

2.4. Difference Scheme for the Poisson Equation for Electric Field Potential

The difference scheme for problem (12)–(11) can be written as

$$-\frac{\varphi^s_{l-1} - 2\varphi^s_l + \varphi^s_{l+1}}{h^2} = \frac{q_e}{\varepsilon_0}\Big(n^s_{+,l} + n^s_{2+,l} - n^s_{e,l}\Big), \quad s > 0, \quad 1 \le l \le M-1,$$
$$\varphi^s_0 = 0, \quad \varphi^s_M = V_a\sin(\omega s\tau), \quad s > 0.$$

2.5. Difference Scheme for the Problem of Balance of the Concentration of Metastable Atoms

At $s > 0$ and $2 \le l \le M-2$, the difference scheme for problem (13)–(15) can be written as

$$h\frac{n^s_{m,l}-n^{s-1}_{m,l}}{\tau}-\left(D^{s-1}_{m,l+1/2}\frac{n^s_{m,l+1}-n^s_{m,l}}{h}-D^{s-1}_{m,l-1/2}\frac{n^s_{m,l}-n^s_{m,l-1}}{h}\right)$$
$$=h\Big(R^{s-1}_{6,l}n^s_{e,l}N^{s-1}_l+R^{s-1}_{18,l}n^s_{e,l}n^{s-1}_{2^*,l}-R^{s-1}_{3,l}n^s_{m,l}n^s_{e,l}-R^{s-1}_{7,l}n^s_{m,l}-R^{s-1}_{8,l}N^{s-1}_l n^s_{m,l}$$
$$-R^{s-1}_{9,l}n^s_{m,l}n^s_{e,l}-R^{s-1}_{10,l}\Big(n^s_{m,l}\Big)^2-R^{s-1}_{15,l}\Big(N^{s-1}_l\Big)^2n^s_{m,l}-R^{s-1}_{18,l}n^s_{e,l}n^{s-1}_{2^*,l}-R^{s-1}_{17,l}n^s_{m,l}n^{s-1}_{2^*,l}$$
$$-R^{s-1}_{19,l}n^s_{m,l}\Big(N^{s-1}_l\Big)^2-\Big(R^{s-1}_{2,l}+R^{s-1}_{10,l}\Big)\Big(\Big(n^{s-1}_{m,l}\Big)^2+2n^{s-1}_{m,l}\Big(n^s_{m,l}-n^{s-1}_{m,l}\Big)\Big)\Big).$$

Boundary conditions (14)–(15) are approximated as follows. At $s > 0$ and $l = 1$, we have

$$h\frac{n^s_{m,1}-n^{s-1}_{m,1}}{\tau}-D^{s-1}_{m,3/2}\frac{n^s_{m,2}-n^s_{m,1}}{h}-\frac{1}{4}n^s_{m,1}\sqrt{8kT_{a,1}/\pi m_a}$$
$$=h\Big(R^{s-1}_{6,1}N^{s-1}_1n^s_{e,1}-R^{s-1}_{7,1}n^s_{m,1}+R^{s-1}_{18,1}n^s_{e,1}n^s_{2^*,1}-R^{s-1}_{3,1}n^s_{m,1}n^s_{e,1}-R^{s-1}_{8,1}n^s_{m,1}N^{s-1}_1$$
$$-R^{s-1}_{9,1}n^s_{m,1}n^{s-1}_{e,1}-\Big(R^{s-1}_{2,1}+R^{s-1}_{10,1}\Big)\Big(\Big(n^{s-1}_{m,1}\Big)^2+2n^{s-1}_{m,1}\Big(n^s_{m,1}-n^{s-1}_{m,1}\Big)\Big)$$
$$-R^{s-1}_{15,1}\Big(N^{s-1}_1\Big)^2n^s_{m,1}-R^{s-1}_{17,1}n^s_{m,1}n^{s-1}_{2^*,1}-R^{s-1}_{19,1}n^s_{m,1}\Big(N^{s-1}_1\Big)^2\Big).$$

At $s > 0$ and $l = M-1$, we have

$$h\frac{n^s_{m,M-1}-n^{s-1}_{m,M-1}}{\tau}+D^{s-1}_{m,M-3/2}\frac{n^s_{m,M-1}-n^s_{m,M-2}}{h}-\frac{1}{4}n^s_{m,M-1}\sqrt{8kT_{a,M-1}/\pi m_a}$$
$$=h\Big(R^{s-1}_{6,M-1}N^{s-1}_{M-1}n^s_{e,M-1}-R^{s-1}_{7,M-1}n^s_{m,M-1}+R^{s-1}_{18,M-1}n^s_{e,M-1}n^s_{2^*,M-1}$$
$$-R^{s-1}_{3,M-1}n^s_{m,M-1}n^s_{e,M-1}-R^{s-1}_{8,M-1}n^s_{m,M-1}N^{s-1}_{M-1}-R^{s-1}_{9,M-1}n^s_{m,M-1}n^{s-1}_{e,M-1}$$
$$-\Big(R^{s-1}_{2,M-1}+R^{s-1}_{10,M-1}\Big)\Big(\Big(n^{s-1}_{m,M-1}\Big)^2+2n^{s-1}_{m,M-1}\Big(n^s_{m,M-1}-n^{s-1}_{m,M-1}\Big)\Big)$$
$$-R^{s-1}_{15,M-1}\Big(N^{s-1}_{M-1}\Big)^2n^s_{m,M-1}-R^{s-1}_{17,M-1}n^s_{m,M-1}n^{s-1}_{2^*,M-1}-R^{s-1}_{19,M-1}n^s_{m,M-1}\Big(N^{s-1}_{M-1}\Big)^2\Big).$$

2.6. Difference Scheme for the Kinetic Equation for Argon Dimers Ar^*_2

At $s > 0$ and $2 \le l \le M-2$, the difference scheme for Eq (16) has the form

$$\frac{n^s_{2^*,l}-n^{s-1}_{2^*,l}}{\tau}=R^{s-1}_{19,l}n^s_{m,l}\Big(N^{s-1}_l\Big)^2+R^{s-1}_{15,l}n^s_{m,l}\Big(N^{s-1}_l\Big)^2-R^{s-1}_{14,l}n^s_{2^*,l}$$
$$-R^{s-1}_{16,l}\Big(\Big(n^{s-1}_{2^*,l}\Big)^2+2n^{s-1}_{2^*,l}\Big(n^s_{2^*,l}-n^{s-1}_{2^*,l}\Big)\Big)-R^{s-1}_{17,l}n^s_{m,l}n^s_{2^*,l}-R^{s-1}_{18,l}n^s_{e,l}n^s_{2^*,l}.$$

2.7. Difference Scheme for the Kinetic Equation for Neutral Atoms

At $s > 0$ and $1 \le l \le M-1$, the difference scheme for Eq. (17) has the form

$$\frac{N^s_l-N^{s-1}_l}{\tau}=-R^{s-1}_{1,l}n^s_{e,l}N^s_l+R^{s-1}_{2,l}\Big(n^s_{m,l}\Big)^2+R^{s-1}_{4,l}n^s_{+,l}n^s_{e,l}+R^{s-1}_{7,l}n^s_{m,l}$$
$$-R^{s-1}_{5,l}\Big(n^s_{e,l}\Big)^2n^s_{+,l}-R^{s-1}_{6,l}N^s_ln^s_{e,l}+R^{s-1}_{13,l}n^s_{e,l}n^s_{2+,l}+\Big(R^{s-1}_{19,l}-R^{s-1}_{15,l}\Big)n^s_{m,l}$$
$$+R^{s-1}_{13,l}n^s_{e,l}n^s_{2+,l}+2N^{s-1}_l\Big(N^s_l-N^{s-1}_l\Big)+R^{s-1}_{12,l}n^s_{e,l}n^s_{2+,l}+R^{s-1}_{14,l}n^s_{2^*,l}$$
$$+\Big(R^{s-1}_{19,l}-R^{s-1}_{15,l}\Big)n^s_{m,l}\Big(\Big(N^{s-1}_l\Big)^2+2N^{s-1}_l\Big(N^s_l-N^{s-1}_l\Big)\Big)$$
$$+R^{s-1}_{16,l}n^s_{2^*,l}+R^{s-1}_{17,l}n^s_{2^*,l}n^s_{m,l}.$$

2.8. Difference Scheme for the Equation of Thermal Conductivity of Atomic-Ion Temperature

The averaged parameters entering into Eq. (19) are calculated using (to approximate the integrals entering into (18)-type expressions) the quadrature formulas of left rectangles:

$$\widehat{n}^p_{e,l} = \frac{1}{L_t} \sum_{s=(p-1)L_T+1}^{pL_T} n^s_{e,l}.$$

Similarly, we approximate $\widehat{j}^p_i$, $\widehat{E}^p$, $\widehat{Q}^p_{\rm el}$, and $\widehat{N}^p$. Then, at $1 \le l \le \le M-1$, the difference scheme for problem (19) has the form

$$-\left(\lambda_{a,l+1/2}\frac{T_{a,l+1}-T_{a,l}}{h} - \lambda_{a,l-1/2}\frac{T^s_{a,l}-T_{a,l-1}}{h}\right) = h\Big(\widehat{Q}^p_{{\rm el},l}\widehat{n}^p_{e,l}N^p_l + \widehat{j}^p_{i,l}\widehat{E}^p_l\Big).$$

Boundary conditions (20) are approximated as follows. At $l=0$, we have

$$-\left(\lambda_{a,3/2}\frac{T_{a,2}-T_{a,1}}{h} - \chi\Big(T_{a,0}-T_{\rm W}\Big)\right) = h\Big(\widehat{Q}^p_{{\rm el},1}\widehat{n}^p_{e,1}N^p_1 + \widehat{j}^p_{i,1}\widehat{E}^p_1\Big).$$

At $l=M$, we have

$$-\left(-\chi\Big(T_{a,M}-T_{\rm W}\Big) - \lambda_{a,M-3/2}\frac{T_{a,M-1}-T_{a,M-2}}{h}\right)$$
$$= h\Big(\widehat{Q}^p_{{\rm el},M-1}\widehat{n}^p_{e,M-1}N^p_{M-1} + \widehat{j}^p_{i,M-1}\widehat{E}^{M-1}_1\Big).$$

3. CALCULATION OF THE DENSITY OF CHARGED PARTICLE FLUXES

A key parameter of each particular plasmatron is the volt–ampere characteristic: the relationship between the total current through the gas-discharge interval and the voltage across it, derived from either field experiments or numerical calculations. The total current $j(t) = q_e(G_+ + G_{2+} - G_e) + \varepsilon_0 \partial E/\partial t$ passing through the gas-discharge interval consists of the conduction current $q_e(G_+ + G_{2+} - G_e)$ and the bias current $\varepsilon_0 \partial E/\partial t$. The calculation of the conduction current requires the calculation of the density of charged particle fluxes. The density of ion fluxes averaged over the period also enters into the right-hand side of the equation for atomic-ion temperature. At high gradients of the solution and coefficients of the balance equations for charged particles, the simple numerical differentiation leads to a significant error in the calculated density of charged particle fluxes and the flux sweep method cannot be used with directional differences; therefore, we modify the Hummel method to calculate the flux [32]. The modification proposed by us implies the calculation of (1) charged particle concentrations using the implicit difference scheme constructed in subsections 2.1–2.3 of this paper and (2) the density of the charged particle flux from the already known concentration of particles, taking into account the fact that the mobility coefficients depend on the reduced local field. This sequence of calculations allows us to avoid the limitation on the time step associated with the Courant condition.

4. NUMERICAL SOLUTION OF MODEL PROBLEMS AND ANALYSIS OF RESULTS

The RFC-discharge at increased pressures has been studied relatively little. At atmospheric pressure and an interelectrode distance of 0.2 cm, the maximum experimental density of electrons in the center of the discharge is 5×10^{11} cm^{-3} and the calculated density of electrons and ions in the ambipolar region is $\approx 7 \times 10^{11}$ cm^{-3} [34]. The calculations using our model under the same conditions revealed a maximum concentration of $\approx 3.9 \times 10^{11}$ (Fig. 1). The profile of the spatial distribution of charged particles between electrodes qualitatively coincides with that obtained in the computational study [35]. The quantitative difference of our results from those obtained in [35] is explained by a higher voltage used in [35].

Also, calculations have been performed for the model problem at atmospheric pressure, an interelectrode distance of 0.2 cm, and an amplitude of the applied voltage of 100 V. The period-averaged charged particle densities are shown in Fig. 2. The calculations have indicated that the densities of molecular ions of Argon increase in near-electrode regions and the quasi-neutrality is retained. This

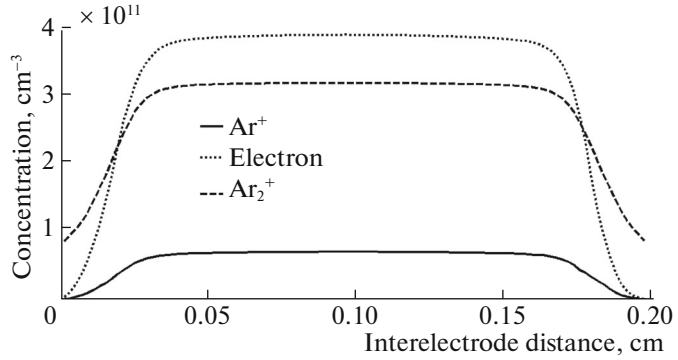

Fig. 1. Profile of the averaged concentration of charged particles at an interelectrode distance of 0.2 cm.

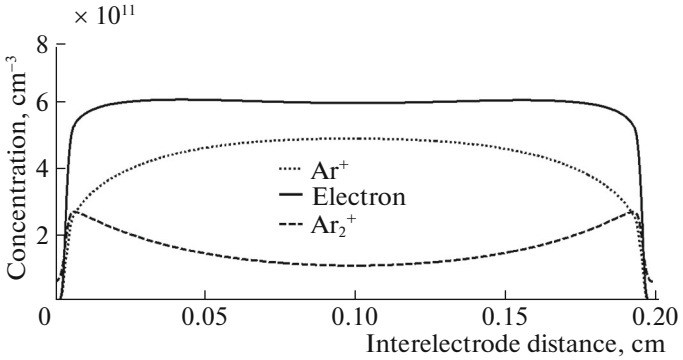

Fig. 2. Profile of the averaged concentration of charged particles at an interelectrode distance of 2 cm.

effect is associated with a larger gas temperature at the center of the discharge in comparison with the near-electrode region as well as with the fact that the coefficients of plasmachemical processes involving heavy particles depend on gas temperature (see Table 1). According to the calculations, the density of atomic ions exceeds the dimer density approximately 2.5 times; in this case, the minimum concentration of dimers is observed at the center of the discharge, while the near-electrode regions are characterized by a concentration increase. The profile of atomic ions has two symmetrical local maxima close to near-electrode regions.

CONCLUSIONS

In this study, we have proposed a mathematical model of an RFC-discharge between symmetrical electrodes in the local approximation at atmospheric pressure. The model incorporates electrons, atomic and molecular ions, metastable atoms, atoms in the ground state, and Argon dimers (the model includes a total of twenty plasmachemical reactions). A simplified scheme of the Argon atom has been used, where the four lowest closely spaced electronically excited states (two metastable and two resonant states) are replaced by a single level. The mathematical model includes a convection–diffusion equation for an electron gas, convection–diffusion equations for atomic and molecular ions, Poisson's equation for the electric field potential, a balance equation for the concentration of metastable atoms, a kinetic equation for Argon dimers, and a heat conduction equation for an atomic-ion gas.

Difference schemes have been constructed for initial, boundary, and initial–boundary value problems entering into the nonlinear system describing the process of RFC-discharge under consideration.

The results of numerical calculations at atmospheric pressure and an interelectrode distance of 0.2 cm were compared with existing experimental and calculated data taken from other literature sources. In addition, the results of calculations for an interelectrode distance of 2 cm have beeb presented and their results have beeb analyzed.

The results of numerical simulations have indicated that if the gas is significantly heated (at increased pressures and for large interelectrode distances at low pressures), the change in the gas temperature in the interelectrode space essentially affects the ratio between contributions to the formation and destruction of particles in different plasmachemical processes and, consequently, affects the distribution and fraction of charged (electrons, and atomic and molecular ions) and excited particles in the discharge interval, which determines the discharge evolution.

ACKNOWLEDGMENTS

The work is performed according to the Russian Government Program of Competitive Growth of Kazan Federal University. The publication was carried out with the financial support of the Russian Foundation for Basic Research (projects nos. 16-01-00301, 16-31-00378).

REFERENCES

1. *Essays on Physics and Chemistry Low-Temperature Plasma,* Ed. by L. S. Polak (Nauka, Moscow, 1971) [in Russian].
2. *Low-Temperature Plasma,* Vol. 3: *Plasma Chemistry,* Ed. by L. S. Polak and Yu. A. Lebedev (Nauka, Novosibirsk, 1991) [in Russian].
3. A. Fridman, *Plasma Chemistry* (Cambridge Univ. Press, Cambridge, 2008).
4. R. Ouelette, M. Barbier, P. Cheremisinoff, et al., *Low Temperature Plasma Technology Applications* (Ann Arbor Science, Ann Arbor, MI, 1980; Energoatomizdat, Moscow, 1983).
5. A. L. Mosse and I. O. Burov, *Treatment of Dispersed Materials in Plasma Reactors* (Nauka Tekhnika, Minsk, 1980) [in Russian].
6. N. V. Tikhonova, V. S. Zheltukhin, V. Yu. Chebakova, and I. A. Borodaev, "Mathematical model of high-frequency plasma processing of multilayer materials uppers," Vestn. Kazan. Tekhnol. Univ. **15** (17), 36–39 (2012).
7. I. Sh. Abdullin, V. S. Zheltukhin, and N. F. Kashapov, *High Frequency Plasma-Jet Processing of Materials at Lower Pressures. The Theory and Application Practice* (Kazan. Univ., Kazan', 2000) [in Russian].
8. V. S. Zheltukhin, V. Yu. Chebakova, and M. N. Shneider, "Simulation of HFC-discharge at large interelectrode distances," in *Proceedings of the 9th All-Russia Conference on Grid Methods for Boundary Problems and Applications* (Otechestvo, Kazan', 2012), pp. 183–186.
9. I. B. Badriev, V. S. Zheltukhin, and V. Yu. Chebakova, "On solution of some nonlinear boundary and initial-boundary value problems," in *Proceedings of the 22nd International Symposium on Dynamical and Technological Problems of Mechanics of Construction and Continuous Media* (TRP, Moscow, 2016), pp. 31–33.
10. V. P. Savinov, *Physics of High-Frequency Capacitive Discharge* (Fizmatlit, Moscow, 2013) [in Russian].
11. Yu. P. Raizer, M. N. Shneider, and N. A. Yatsenko, *High-Frequency Capacitive Discharge: Physics, Experiment Technique. Applications* (Mosk. Fiz. Tekhnol. Inst., Moscow, 1995) [in Russian].
12. P. Chebert and N. Braithwaite, *Physics of Radio-Frequency Plasmas* (Cambridge Univ. Press, Cambridge, 2011).
13. Yu. P. Raizer, *Gas Discharge Physics* (Springer, Berlin, 1991; Intellekt, Dolgoprudnyi, 2009).
14. Yu. A. Lebedev, A. V. Tatarinov, A. Yu. Titov, and I. L. Epshtein, "Two-dimensional model of a non-equilibrium strongly non-uniform microwave discharge in a DC external field," Uchen. Zap. Kazan. Univ., Ser. Fiz.-Mat. Nauki **156** (4), 120–132 (2014).
15. V. Yu. Chebakova, V. S. Zheltukhin, "On mathematical models of high frequency capacitive discharge," in *Proceedings of the 10th All-Russia Conference on Grid Methods for Boundary Problems and Applications,* Tr. Mat. Tsentra Lobachevskogo (Otechestvo, Kazan', 2013), pp. 98–128.
16. I. Sh. Abdullin, V. S. Zheltukhin, and V. Yu. Chebakova, "High frequency capacitive discharge: simulation (review)," Vestn. Kazan. Tekhnol. Univ. **17** (23), 9–14 (2014).
17. E. Castonos. Martinez, Y. Kabouzi, K. Makasheva, and M. Moisan, "Modeling of microwave-sustained plasmas at atmospheric pressure with application to discharge contraction," Phys. Rev. E **70**, 066405 (2004). doi 10.110/PhysPevE.70.066405
18. V. Yu. Chebakova, "Numerical simulation of the high frequency capacitive discharge," Uch. Zap. Kazan. Univ., Ser. Fiz.-Mat. Nauki **157** (2), 126–140 (2015).
19. I. Sh. Abdullin, V. S. Zheltukhin, M. N. Shneider, and V. Yu. Chebakova, "Simulation of high frequency capacitive discharge in argon with account of heating of heavy particles," Mat. Metody Tekh. Tekhnol. **5**, 34–37 (2014).
20. I. Sh. Abdullin, V. S. Zheltukhin, V. Yu. Chebakova, and M. N. Shneider, "Non-stationary model of HFC-discharge at lower pressure ," in *Proceedings of the 10th All-Russia Conference on Grid Methods for Boundary Problems and Applications* (Kazan. Univ., Kazan', 2014), pp. 15–20.

21. D. Kh. Bikchantaev, V. S. Zheltukhin, and V. Yu. Chebakova, "Numerical study of interaction process between high frequency capacitive discharge with materials," in *Proceedings of the All-Russia Conference on Control Theory and Mathematical Modeling* (Udmurtskii Univ., Izhevsk, 2015), pp. 241–242.
22. I. B. Badriev, "On the solving of variational inequalities of stationary problems of two-phase flow in porous media," Appl. Mech. Mater. **392**, 183–187 (2013). doi 10.4028/www.scientific.net/AMM.392.183
23. I. B. Badriev and L. A. Nechaeva, "Mathematical simulation of steady filtration with multivalued law," PNRPU Mech. Bull. **3**, 37–65 (2013).
24. I. B. Badriev and M. M. Karchevskii, "Convergence of an iterative process in a Banach space," J. Math. Sci. **71**, 2727–2735 (1994).
25. I. Badriev and V. Banderov, "Numerical method for solving variation problems in mathematical physics," Appl. Mech. Mater. **668–669**, 1094–1097 (2014).
26. I. B. Badriev, V. V. Banderov, M. V. Makarov, and V. N. Paimushin, "Determination of stress-strain state of geometrically nonlinear sandwich plate," Appl. Math. Sci. **9** (77–80), 3887–3895 (2015).
27. A. A. Kudryavtsev, A. S. Smirnov, and L. D. Tsendin, *Physics of Glow Discharge* (Lan', St. Petersburg, 2010) [in Russian].
28. C. M. Ferreira, J. Loureiro, and A. Ricard, "Populations in the metastable and the resonance levels of argon and stepwise ionization effects in a low-pressure argon positive column," J. Appl. Phys. **57** (82), 82–90 (1985). doi: 10.1063/1.335400.
29. N. A. Dyatko, Yu. Z. Ionikh, A. V. Meshchanov, and A. P. Napartovich, "Study of the dark phase in the initial stage of the positive column formation in an argon glow discharge," Plasma Phys. Rep. **31**, 871–885 (2005).
30. G. J. M. Hagelaar, F. J. de Hoog, and G. M. W. Kroesen, "Boundary conditions in fluid models of gas discharges," Phys. Rev. E **62**, 1452–1454 (2000).
31. G. J. M. Hagelaar and L. C. Pitchford, "Solving the Boltzmann equation to obtain electron transport coefficients and rate coefficients for fluid models," Plasma Sources Sci. Technol. **14**, 722–733 (2005).
32. P. Lymberopoulos Dimitris and J. Economou Demetre, "Fluid simulations of glow discharge and effect of metastable atoms in argon," J. Appl. Phys. **73**, 3668–3679 (1993).
33. Zhu Xi-Ming and Pu Yi-Kang, "Modeling of microwave- sustained plasmas at atmospheric pressure with application to discharge contraction," J. Phys. D: Appl. Phys. **43**, 015204 (2010). doi 10.1088/0022-3727/43/1/015204
34. N. P. Balcon, A. Aanesland, G. J. M. Hagelaar, R. Boswell, and J. P. Boeuf, "Atmospheric pressure RF discharge in argon: optical diagnostic, fluid model and applications," in *Proceedings of the 28th International Conference on Phenomena in Ionized Gases ICPIG, Prague, Czech Republic, 2007,* p. 957–960.
35. N. P. Balcon, G. J. M. Hagelaar, and J. P. Boeuf, "Numerical model of an argon atmospheric pressure RF discharge," IEEE Trans. Plasma Sci. **36**, 2782–2787 (2008).
36. M. Moravej, X. Yang, R. F. Hicks, J. Penelon, and S. E. Babayan, "A radio-frequency nonequilibrium atmospheric pressure plasma operating with argon and oxygen," J. Appl. Phys. **99**, 093305-1–6 (2006). doi 10.1063/1.2193647
37. I. L. Epstein, M. Gavrilović, S. Jovircević, N. Konjević, Yu. A. Lebedev, and A. V. Tatarinov, "The study of a homogeneous column of argon plasma at a pressure of 0.5 torr, generated by means of the Beenakker's cavity," Eur. Phys. J. D **68**, 334-1–9 (2014). doi 10.1140/epjd/e2014-50182-7
38. E. Karoulina and Yu. Lebedev, "Computer simulation of microwave and DC plasmas comparative characterization of plasmas," J. Phys. D: Appl. Phys. **25**, 401–412 (1992).
39. B. M. Smirnov, "Modeling of gas discharge plasma," Phys. Usp. **52**, 559–571 (2009).
40. B. M. Smirnov, "Diffusion and mobility of ions in a gas," Sov. Phys. Usp. **10**, 313–331 (1967).
41. V. G. Fastovskii, A. E. Rovinskii, and Yu. V. Petrovskii, *Inert Gases* (Atomizdat, Moscow, 1972; Israel Program for Scientific Translations, Jerusalem, 1967).
42. E. McDaniel, *Collision Phenomena in Ionized Gases* (Wiley, New York, 1964).
43. J. P. Boeuf and L. C. Pitchford, "Two-dimensional model of a capacitively coupled RF discharge and comparisons with experiments in the Gaseous Electronics Conference reference reactor," Phys. Rev. E **51**, 1376–1390 (1995).
44. B. M. Smirnov, *Excited Atoms* (Energoizdat, Moscow, 1982) [in Russian].
45. B. Bora, H. Bhuyan, M. Favre, E. Wyndham, and H. Chuaqui, "Diagnostic of capacitively coupled low pressure radio frequency plasma: an approach through electrical discharge characteristic," Int. J. Appl. Phys. Math. **1**, 124–128 (2011).
46. R. P. Fedorenko, *Introduction to Computational Physics* (Mosk. Fiz. Tekhnol. Inst., Moscow, 1994) [in Russian].
47. A. A. Kulikovsky, "A more accurate scharfetter-gummel algorithm of electron transport for semiconductor and gas discharge simulation," J. Comput. Phys. **119**, 149–155 (1995).